

Neutron Facilities of the DARIA Compact Neutron Source: Parameters and Features

S. V. Grigoriev^{a, b, *}, N. A. Kovalenko^b, K. A. Pavlov^{a, b}, E. V. Moskvina^{a, b},
V. G. Syromyatnikov^{a, b}, and N. A. Grigoryeva^a

^a St. Petersburg State University, St. Petersburg, 199034 Russia

^b Konstantinov Petersburg Nuclear Physics Institute, National Research Centre “Kurchatov Institute,”
Gatchina, Leningrad oblast, 188300 Russia

*e-mail: grigoryev_sv@pnpi.nrcki.ru

Received May 22, 2023; revised June 19, 2023; accepted July 28, 2023

Abstract—The DARIA compact accelerator-driven neutron sources, based on a linear proton accelerator, is designed to create neutron beams for a diffractometer, reflectometer, and small-angle scattering facility. The experimental facilities are optimized in momentum transfer range, instrumental resolution, geometric dimensions, the repetition rate and duration of neutron pulses.

DOI: 10.3103/S1062873823703690

INTRODUCTION

The most popular group of neutron research methods is neutron scattering in condensed matter physics. Due to the unique combination of properties of thermal neutrons—the absence of electric charge, presence of a magnetic moment, and characteristic values of the de Broglie wavelength (1–10 Å) and energy (1–25 meV)—they are used to study the structure of matter, the nature of magnetic phenomena, and the dynamics on the atomic and molecular scales.

Compact accelerator-driven neutron sources (CANS) are a modern trend in research techniques using neutron scattering. CANS are understood as low-power neutron sources operating on the basis of pulsed ion or electron accelerators and reaching a neutron beam intensity per pulse of up to 10^{15} n s⁻¹ cm⁻² [1–8]. CANS for condensed matter physics research are equipped with a target, neutron moderator, and neutron guide system, which makes it possible to place several neutron facilities on a single target. Beryllium or lithium are used more frequently as targets, since the binding energy of neutrons in the nucleus of these elements is low. The target of the compact source is equipped with different types of moderators for thermalization of the obtained neutrons, which ensures an average flux in the thermal neutron beam Φ of about 10^{12} n s⁻¹ cm⁻² at the target assembly output. If transport losses are minimized, then this neutron flux is sufficient for the diffraction, reflectometric, small-angle, and radiographic studies.

A compact neutron source is initially inferior (by several orders of magnitude of the neutron flux) to a large accelerator-type source or a high-flux nuclear

reactor, but a significant amount of these losses can be compensated by increasing the capture aperture and deep optimization of the experimental facility, including adaptation of the parameters of the accelerator, target, and moderator to the needs of each neutron instrument. For example, the expected thermal neutron flux density in the moderator of high-flux reactors with a capacity of tens of MW is 10^{14} n s⁻¹ cm⁻², while for the CANS DARIA (Dedicated for Academic Research and Industrial Application) prototype it is 10^{12} n s⁻¹ cm⁻². When comparing Φ , it should be taken into account that a narrow spectral line is cut out of the total neutron flux at stationary reactor facilities, i.e., from 90 to 99% of neutrons are ejected from the flux. In the case of pulsed sources (an example of which is the CANS), almost all the neutrons in a pulse are used in the study, since the neutrons scattered on the sample are detected by the time-of-flight technique.

Existing and projected compact neutron sources can be conditionally divided into two classes. The first one includes the university-type sources intended for teaching students and conducting scientific research which do not require a high luminosity or a development of new neutron techniques. The second class includes medium-power sources, for which, when performing the complete joint optimization of all elements of a compact source, it is possible to achieve a luminosity on a sample which is not inferior to that of modern reactors of medium and even high power. Similar sources are applied as common use centers.

In the wake of worldwide interest in compact neutron sources, we present a Russian initiative to create a similar source—the project of a compact neutron source Dedicated to Applied Research and Industrial

Application (DARIA). The DARIA CANS, designed for applied research and industrial applications, is equipped with three time-of-flight neutron facilities: a neutron powder diffractometer, a polarized neutron reflectometer, and a small-angle neutron scattering facility [9].

The simulation of the DARIA CANS target assembly was carried out by the Monte Carlo method in the PHITS software package [10]. A pulsed proton flux with an energy of 13 MeV, by hitting the target, creates a pulsed neutron flux. This flux after passing through the cold moderator is characterized by the neutron pulse duration τ and the neutron pulse repetition rate f . For the DARIA CANS, the average τ and f values are about 100 μs and 100 Hz, respectively. In this case, each neutron pulse has a wide spectral distribution from 1 to 12 \AA . Therefore, the pulse repetition rate should correspond to the range of the applied spectrum of neutrons to avoid the distortion of the obtained data on the detector due to the phenomenon of “pulse overlap,” when the fastest neutrons from the subsequent neutron pulse overtake the slowest neutrons from the previous pulse. The f value for which there is no pulse overlap is determined by the time-of-flight base L and width of the neutron spectrum $\Delta\lambda$ for a specific research facility.

The neutron guide systems were simulated by the Monte Carlo method in the McStas software package [11]. To ray-trace neutrons, a model is created that sequentially simulates the operation of all station nodes that directly affect the profile of the neutron beam used: a source model with the time-depending generation and high-aperture characteristics, an optical path, a cascade of choppers, and a time-resolved detector. Physical parameters of the nodes are determined based on the achievement of maximum luminosity of the device, under condition of a satisfactory instrumental resolution. The parameters of neutron facilities and the neutron flux Φ at the sample position are presented in [12–14] and are compared there with the parameters of similar facilities and neutron fluxes Φ at the IBR-2 pulsed reactor of the Laboratory of Neutron Physics of the Joint Institute for Nuclear Research (JINR) in Dubna.

COMPACT NEUTRON SOURCE: SCHEMATIC DIAGRAM

The main components of the DARIA CANS are a pulsed proton accelerator, a target assembly, and neutron scattering instruments. A proton accelerator, consisting of a source based on the electron–cyclotron resonance and accelerating structures, ensures the formation of a pulsed beam structure on the beryllium target with a high peak current up to 100 mA and a frequency up to 200 Hz [15, 16]. The proton energy is limited from above by 13 MeV due to the undesirable generation of tritium in the target at high proton energies. To obtain neutrons, the collision reaction of pro-

tons with beryllium nuclei is used, which provides a neutron yield sufficient for studies in the condensed matter physics, with a moderate heat release [4, 5]. The compact dimensions of the target (about 5 cm in diameter and 1.1 mm in thickness) will provide a relatively high density of the neutron flux Φ [17]. Small dimensions of the target and the thermal moderator placed around the target stipulate also the compact biological protection. A cooling system is being developed, which is designed to remove about 30 kW of the average heat release from the target and its environment. With the above parameters of the accelerator and target, it is possible to achieve a neutron flux density per pulse up to $5 \times 10^{12} \text{ n s}^{-1} \text{ cm}^{-2}$. Neutron facilities are optimized together with their respective neutron moderators. A specific list of neutron stations is determined by the needs of the research center. Therefore, the DARIA CANS incorporates the concept of flexible change of neutron source parameters: the moderator temperature, the repetition rate and duration of neutron pulses.

POWDER NEUTRON DIFFRACTOMETER

The neutron diffractometer is designed to determine the crystalline and magnetic structures of solids. Parameters of the time-of-flight diffractometer for DARIA CANS are optimized with respect to a maximum flux at a given resolution. For the optimal resolution-to-luminosity ratio, the range of neutron wavelengths, the frequency and duration of the pulses are determined. A time-of-flight diffractometer with a flight path $L = 23.5 \text{ m}$ is schematically shown in Fig. 1. The operating spectral range is $\lambda = 1\text{--}5 \text{ \AA}$, the resolution $\Delta d/d = 0.005$, and neutron pulse length $\Delta\tau = 30 \mu\text{s}$.

From the neutron moderator in the target assembly 1, neutrons are extracted into the neutron guide hall through a straight neutron guide 2 with a cross section of $20 \times 50 \text{ mm}^2$ and length of 1.5 m. A chopper consisting of two disks rotating synchronously towards each other is used to generate a time-symmetric pulse. In the diffractometer scheme, the first pair of choppers 3 is designed to link the reference point to the time-of-flight base. The second pair of disk choppers 5, located at a distance of 5.5 m from the moderator, is designed for the pulse overlap elimination and the spectral band narrowing to improve a resolution.

The neutron guide system 4 with a length of 3.9 m is installed between disk choppers 3 and 5 to reduce neutron flux losses; in this case, a part of the background from fast neutrons and gamma radiation is cut off by the first disk chopper 3. After the second disk chopper 5, a curved neutron guide 6 with a length of 17 m is installed, which makes it possible to escape from the target line-of-sight and to get rid of the remaining fast neutrons and gamma radiation. Neutron guides 4 and 6 are assembled from straight sec-

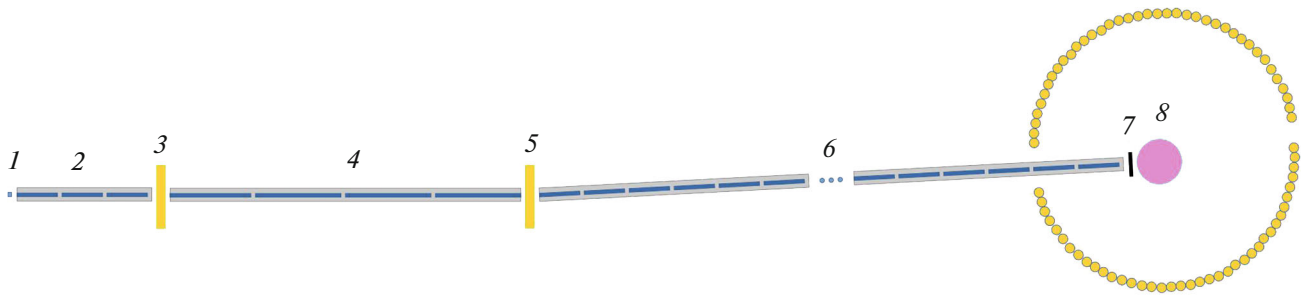


Fig. 1. Schematic diagram of neutron powder diffractometer (see description in text).

tions with supermirrors of length $l = 0.5$ m and have the same parameters: the cross-section of 20×50 mm² and the $m = 2$ supermirror coating. The rotation of the sections relative to each other in the curved neutron guide 6 is $\alpha = \arctan(l/\rho) = 0.00795^\circ$, for the radius of curvature $\rho = 3601.5$ m. Behind the neutron guide, directly in front of the sample assembly 8, a diaphragm 7 with a variable aperture is installed to additionally limit the neutron beam divergence and reduce the background on the detector. After scattering on the sample, the neutrons fall on the detector group 9 located at a distance of 1.5 m from the sample within a range of scattering angles 2θ from $\pm 10^\circ$ to $\pm 170^\circ$. The group is divided into separate sectors of 10° – 20° .

Parameters of the neutron diffractometer for DARIA CANS are presented in Table 1. For comparison, the characteristics of the RTD diffractometer at JINR are also given there [18]. The similarities and differences between the two diffractometers are obvious. The instrument geometry (flight base, cross-sections of neutron guides, range of scattering angles) can be considered the same. A range of operating wavelengths turns out to be different and, as a result, a range of interplanar spacings, which is much larger for the RTD diffractometer at JINR. If we consider the class of problems solved in the range of $\Delta d/d = 0.5$ – 29 Å, then the neutron flux Φ on the sample turns out to be of the same order for the two devices under discussion at the same resolution. This means that the diffractometers have the same efficiency for this class of problems.

POLARIZED NEUTRON REFLECTOMETER

The time-of-flight neutron reflectometer with a horizontal scattering plane is designed to determine a profile of density of the neutron scattering length deep into the film, due to changes in its structure or magnetization. The reflectometer is aimed at studying the processes of diffusion, sorption, oxidation and other phenomena on surfaces and interfaces of the media in the semiconducting, metallic, polymeric or biological nanostructures. The reflectometer, operating by the time-of-flight method, measures the intensity of reflection from the plane of a neutron beam with a wide spectral distribution depending on the wavelength at a fixed slip angle. An additional option of the reflectometer for DARIA CANS—measurements using both polarized and unpolarized neutrons—significantly expands the scope of materials science problems. The operating range of the reflectometer in terms of neutron wavelengths is 1–7 Å, and for momentum transfer, it is 0.001–0.5 Å⁻¹. A schematic diagram of the neutron reflectometer is shown in Fig. 2.

The removing collimator 2, located close to the moderator surface inside the target assembly, sets the primary beam collimation of ~ 1 mrad in the horizontal plane. The nonmagnetic NiMo/Ti supermirror 3 ($5 \times 80 \times 210$ mm³, $m = 2$) deflects the neutron beam from the axis of the removing collimator and separate the “useful” (thermal and cold) neutrons from gamma quanta and fast neutrons. The angle of deviation of the neutron beam from the axis of the removing collimator is 20 arcmin. A monitor is installed between the removing collimator and the supermirror to determine a change in the intensity of neutrons from the source.

Table 1. Comparison of main parameters of neutron diffractometer for DARIA CANS and RTD diffractometer at JINR [18]

Diffractometer type	Diffractometer for DARIA CANS	RTD diffractometer at JINR
L	24 m	24–26 m
Neutron guide	Supermirror, 20×50 mm, $m = 2$	Mirror, 15×180 mm, Ni
Operating range	$\lambda = 1$ – 5 Å, $\theta = 10^\circ$ – 170° , $d = 0.5$ – 29 Å	$\lambda = 1$ – 18 Å, $\theta = 1^\circ$ – 170° , $d = 0.6$ – 300 Å
Resolution	$\Delta q/q = 0.5\%$	$\Delta q/q = 1$ – 10%
Φ	5×10^6 n s ⁻¹ cm ⁻²	$\sim 10^7$ n s ⁻¹ cm ⁻²

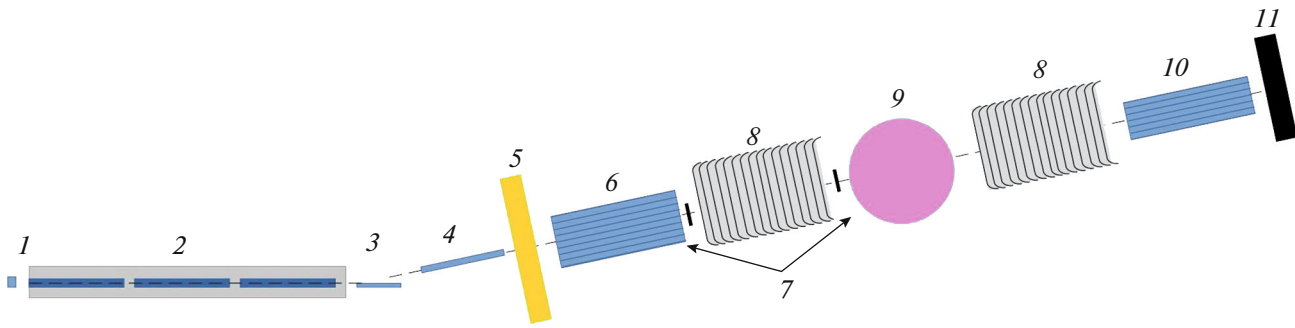


Fig. 2. Schematic diagram of polarized neutron reflectometer (see description in text).

The background collimator ($1 \times 30 \times 400 \text{ mm}^3$) with walls made of steel and borated polyethylene 4 suppresses the residual background from gamma quanta and fast neutrons.

As noted above, the duration τ and frequency f of neutron pulses are set by the CANS proton accelerator. The operating range of wavelengths, with a given neutron flux density on the sample, determines the final choice of the frequency and pulse length of neutrons. A spectrum with a width of $\Delta\lambda$ is cut out using the two-disk chopper 5 from neutron pulses that have a wide spectral distribution exceeding $\Delta\lambda$. For a neutron pulse length $\tau = 100 \mu\text{s}$ and a total length of time-of-flight base $L = 8 \text{ m}$, for a wavelength range $\Delta\lambda = 3 \text{ \AA}$ and a resolution $\Delta\lambda \approx 0.05 \text{ \AA}$, the pulse repetition rate can reach $f = 165 \text{ Hz}$ at a duty factor of 1.66%. If the wavelength range is chosen wider than $\Delta\lambda = 6 \text{ \AA}$, then with the same parameters, the frequency should be no more than $f = 82 \text{ Hz}$ (duty factor 0.83%).

Beam polarizer 6 (a double magnetic supermirror in a constant magnetic field $H \sim 500 \text{ Oe}$) polarizes the neutron beam. When working with nonmagnetic samples, the polarizer is removed from the beam. Collimating diaphragms 7 form the angular divergence of the beam incident on the sample. The radio-frequency adiabatic spin flippers 8 and the analyzer 10 are designed to perform the polarization analysis for magnetic samples. A spin flipper reverses the polarization direction of the neutron spin [19]. As the analyzer, a wide-aperture fan polarizer ($180 \times 250 \times 500 \text{ mm}^3$)

with FeCoV/TiZr supermirror coating of walls [20] is used, which is placed in a magnetic field $H \sim 500 \text{ Oe}$. Close to the analyzer output, the two-coordinate gas position-sensitive detector 11 is installed [21, 22]. An electromagnet and/or a cryostat can be installed in the sample assembly 9. A system of the magnetic guide field is provided in the reflectometer. It is located along the beam from the polarizer magnet to the analyzer magnet.

The neutron reflectometer parameters are given in Table 2; for comparison, the characteristics of the REMUR diffractometer at JINR are also given [18]. The two reflectometers are close in their performance characteristics. The flight base lengths turn out to be different, and as a result, the neutron flux Φ on the sample is significantly (by an order of magnitude) lower for the REMUR reflectometer at JINR.

SMALL-ANGLE NEUTRON SCATTERING FACILITY

The small angle neutron scattering (SANS) facility is a classic point-geometry tool for studying nano- and submicro-scale structures. As a prototype, we consider the YuMO facility at the IBR-2 reactor at the Laboratory of Neutron Physics, JINR [18].

A diagram of the SANS facility on a compact neutron source is shown in Fig. 3. The facility includes such key elements as a cold neutron moderator, a cascade of beam choppers, a neutron guide, a collimation

Table 2. Comparison of main parameters of neutron reflectometer for DARIA CANS and REMUR reflectometer at JINR [18]

Reflectometer type	Reflectometer for DARIA CANS	REMUR reflectometer at JINR
L	8 m	29–34 m
Neutron guide	Supermirror ($m=2$), $1500 \times 10 \times 50 \text{ mm}^3$	Supermirror ($m = 1.2$) conical, $18000 \times 20 \times 160 \text{ mm}^2$
Operating ranges	$\lambda = 1–10 \text{ \AA}$, $q = 0.001–0.5 \text{ \AA}^{-1}$	$\lambda = 0.9–15 \text{ \AA}$, $q = 0.003–0.5 \text{ \AA}^{-1}$
Resolution	$\Delta q/q = 2–10\%$	$\Delta q/q = 3–10\%$
Φ	$10^6 \text{ n s}^{-1} \text{ cm}^{-2}$	$1.6 \times 10^5 \text{ n s}^{-1} \text{ cm}^{-2}$
Detector	Two-coordinate ^3He PSD $250 \times 250 \text{ mm}^2$	Two-coordinate $^3\text{He} + \text{CF}_4$ PSD $178 \times 178 \text{ mm}^2$

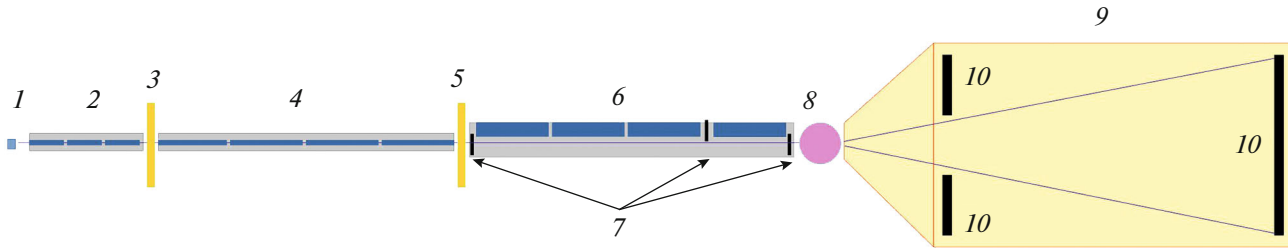


Fig. 3. Schematic diagram of facility for small-angle neutron scattering (see description in text).

system, a sample assembly, and a wide-aperture position-sensitive detector (PSD). Cold moderator 1 provides the primary formation of the neutron beam spectrum, which has an energy maximum in the cold range of spectrum and, preferably, a high brightness in the given direction. The neutron guide section 2 is designed to capture and transport the maximum amount of thermal and cold neutrons in the direction of the sample assembly. The closer this section is to the cold moderator, the higher the neutron flux is on the sample.

The cascade of choppers 3 and 5 creates a clearer pulsed beam structure, roughly specified by the source, and also filters the spectrum to a given wavelength range. The cascade consists of two choppers: chopper 3 is a generator and at the same time a filter of pulse overlap on the detector while chopper 5 is a high-wavelength limiter. The neutron guide path 4 between the choppers ensures the transport of maximum neutron flux to the sample. The collimation system consists of a set of removable collimator/neutron guide sections 6 and several sets of controllable diaphragms of variable size 7 placed in an evacuated volume. The collimation system provides the necessary divergence of the neutron beam on the sample. The sample assembly 8 is a holder of several samples with automated feeding under the neutron beam (for materials science and biology) or a set of devices for creating the external conditions of the experiment: an oven, a cryostat, and a magnet. A wide-aperture position-sensitive neutron detector 10, placed in the evacuated tube 9, consists of two sections, which makes it possible to record the scattering at small and wide angles simultaneously.

As input data for calculations of the neutron flux Φ of the SANS facility, the calculated spectrum of the para hydrogen cold moderator as a part of the target assembly was taken, which was obtained from numerical simulation of the neutron-physical processes occurring in the target. The calculated brightness of the neutron source in the thermal range is about 10^{11} neutrons/($\text{cm}^2 \text{ s sr}$) [17].

A facility is considered that uses only a part of the neutron radiation spectrum. This is a key decision for a low-power source, since makes it possible to maxi-

mize the pulse frequency, and thus to increase the time-averaged power/intensity of the source. With a total length of the facility time-of-flight base $L = 15 \text{ m}$, the neutron pulse duration can reach $\tau = 400 \mu\text{s}$, while the pulse repetition rate $f = 40 \text{ Hz}$ (duty factor 1.6%) can be achieved for the wavelength range $\Delta\lambda = 6 \text{ \AA}$ (2–8 or 6–12 \AA) and the resolution $\Delta\lambda \cong 0.14 \text{ \AA}$. Figure 4 shows the differential neutron flux density at the sample position as a function of wavelength for the 1 m and 5 m collimation and two spectral ranges $\Delta\lambda$ (2–8 or 6–12 \AA). Calculations show that the method can be implemented on a CANS with an aperture ratio of $4 \times 10^7 \text{ n s}^{-1} \text{ cm}^{-2}$ for the collimation scheme of (1 + 1) m and $2 \times 10^6 \text{ n s}^{-1} \text{ cm}^{-2}$ for the collimation scheme of (5+5) m in the momentum transfer range of 3×10^{-3} – 0.5 \AA^{-1} .

The obtained estimates of the luminosity indicate the accessibility of experiments on samples used for work in the field of biology, polymers, medicine, in solid-state research, materials science and metal physics. When studying organic samples, to increase the neutron scattering length density contrast, one should use the deuteration of samples or staining the buffer

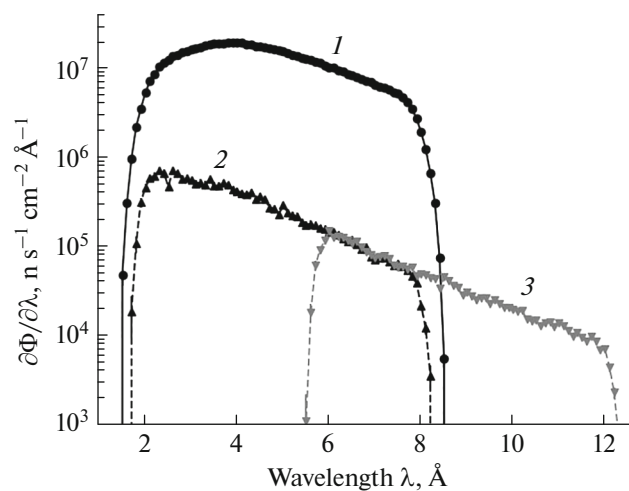


Fig. 4. Differential neutron flux density Φ in sample position depending on neutron wavelength for 1 m (curve 1) and 5 m collimation for two spectral ranges $\Delta\lambda = 2$ –8 \AA (curve 2) and $\Delta\lambda = 6$ –12 \AA (curve 3).

Table 3. Comparison of main parameters of SANS facility for DARIA CANS and YuMO SANS facility at JINR [18]

SANS facility type	SANS facility for DARIA CANS	YuMO SANS facility at JINR
L	18 m	43 m
Neutron guide	Supermirror ($m = 2$), $40 \times 40 \text{ mm}^2$	Supermirror ($m = 1.2$), $30 \times 30 \text{ mm}^2$
Operating ranges	$\lambda = 2\text{--}8 \text{ \AA}$; $6\text{--}12 \text{ \AA}$ $q = 0.005\text{--}0.5 \text{ \AA}^{-1}$	$\lambda = 0.5\text{--}8 \text{ \AA}$ $q = 0.007\text{--}0.7 \text{ \AA}^{-1}$
Resolution	$\Delta q/q = 5\text{--}10\%$	$\Delta q/q = 5\text{--}15\%$
Φ	$10^7 \text{ n s}^{-1} \text{ cm}^{-2}$ (collimation scheme (1 + 1) m); $10^6 \text{ n s}^{-1} \text{ cm}^{-2}$ (collimation scheme (5 + 5) m)	$10^7 \text{ n s}^{-1} \text{ cm}^{-2}$
Detectors	^3He PSD $500 \times 500 \text{ mm}^2$ ^3He PSD $600 \times 600 \text{ mm}^2$	2 PSD ^3He

with a $\text{D}_2\text{O}/\text{H}_2\text{O}$ mixture of heavy and light water. Polarized neutrons can be used to study magnetic inhomogeneities, magnetic structures, and magnetic fluctuations.

The parameters of the small-angle neutron scattering facility for the DARIA CANS are presented in Table 3. For comparison, the characteristics of the YuMO diffractometer at JINR are also given there [18]. The two SANS facilities have the same characteristics. The length of the flight base at the YuMO facility is twice as large as for the SANS facility at the DARIA source, while the neutron flux Φ on the sample in the wavelength range from 2 to 8 \AA is almost the same, therefore the devices have the same operating efficiency.

COMPARISON OF THE PARAMETERS OF NEUTRON FACILITIES

According to the results of numerical simulation of the diffractometer, reflectometer, and SANS facility at CANS, the calculated neutron flux Φ in terms of its values in the sample position is not inferior to the flux Φ for medium-power reactors and pulsed sources, e.g., the IBR-2 pulsed reactor at JINR [18]. The question arises: why does the IBR-2, with a power of 2 MW and a flux in the moderator of thermal neutrons per pulse of $8 \times 10^{15} \text{ n s}^{-1} \text{ cm}^{-2}$, yield the same neutron flux on the sample as the DARIA CANS with the calculated neutron flux density in the moderator per pulse of only $8 \times 10^{12} \text{ n s}^{-1} \text{ cm}^{-2}$? It turns out that compact neutron sources outperform their much more powerful “brothers” in efficiency of production and delivery of thermal and cold neutrons to the sample. Let us demonstrate this.

First, the product of the frequency f and the duration τ of the neutron pulse gives the time-averaged operating parameter for the neutron source—the duty factor. In the case of an IBR-2 pulse source with $f = 5 \text{ Hz}$ and $\tau = 320 \text{ \mu s}$, the duty factor is 0.0016, i.e., the IBR-2 source works during 0.16% of the time. In the case of the DARIA compact pulsed source, for different types of devices, f varies from 40 to 160 Hz and τ ,

from 30 to 400 μs ; in all cases the duty factor is no less than 0.01, which is eight to ten times greater than for the IBR-2. Thus, it is necessary to compare the average neutron flux at the IBR-2 $\Phi = 1.3 \times 10^{13} \text{ n s}^{-1} \text{ cm}^{-2}$ with the average flux in the DARIA CANS moderator, which is $1.6 \times 10^{11} \text{ n s}^{-1} \text{ cm}^{-2}$.

Second, when considering the section S of the neutron extraction channel and the distance h between the channel flange and moderator surface, $\Phi \times 10^{-4} \text{ n/(s cm}^2)$ falls within the channel at the IBR-2 source ($h = 5 \text{ m}$, $S = 10 \times 10 \text{ cm}^2$). For the DARIA CANS ($h = 0.1 \text{ m}$, $S = 3 \times 3 \text{ cm}^2$), $\Phi \times 3 \times 10^{-2} \text{ n/(s cm}^2)$ enters the neutron guide channel, which is hundreds of times greater than at the IBR-2. Consequently, the average neutron fluxes in the channels at the IBR-2 and DARIA CANS are $10^9 \text{ n s}^{-1} \text{ cm}^{-2}$; i.e., the neutron capture efficiency is two orders of magnitude higher in the case of CANS. It should not be forgotten that in the case of a CANS, a significant fraction of captured neutrons has a greater divergence (about 0.3 rad) than necessary for a neutron facility, and therefore will be discarded first by the neutron guides and then also by the collimation system.

Thirdly, the neutron flux density on the sample depends on the length of the time-of-flight base, which provides a time resolution, and on the collimation, which provides a resolution in terms of scattering angle. In a medium-quality neutron guide, the thermal neutron beam loses several percent of intensity per each meter of the neutron guide. If, e.g., the flight base of the reflectometer on the DARIA CANS is 8 m, while the flight base of the REMUR reflectometer on the IBR-2 is 30 m (Table 2), then the neutron flux density Φ on the sample at the DARIA CANS reflectometer will exceed Φ on the REMUR by an order of magnitude, which is shown in Table 2. The geometric arrangement of the neutron facility does not have such significant effect on the neutron flux on the sample, in comparison with the beam collimation. The SANS facilities and diffractometers at the DARIA CANS and the IBR-2 source are identical in their parameters, so the neutron fluxes Φ on the sample are the same, on

the order of 10^6 – 10^7 n s⁻¹ cm⁻². At the same time, one should not forget that medium-class neutron sources ensure the operation of dozens of facilities simultaneously. For example, 16 neutron facilities of various types and purposes operate at the IBR-2.

At a CANS, the number of facilities “feeding on” neutrons from one source is limited to three to four devices due to the compactness of the target and neutron moderator (10^3 cm³). However, in contrast to a medium-power pulsed reactor operating at one frequency f and with one duration τ of a neutron pulse, which makes it necessary to design and construct neutron stations with compromise-based f and τ values instead of optimal ones, three to four devices at the DARIA CANS operate on neutron pulses with adjustable and optimal frequency and duration.

CONCLUSIONS

Thus, the concepts, schematic diagrams, and parameters are presented for three neutron time-of-flight facilities of the DARIA compact neutron source: a powder diffractometer, a polarized neutron reflectometer, and a small-angle neutron scattering facility. The experimental facilities are optimized with respect to the momentum transfer range, instrumental resolution, repetition rate, and duration of neutron pulses. It is shown that compact neutron sources outperform their much more powerful “brothers” by three orders of magnitude in the efficiency of production and delivery of thermal and cold neutrons to the sample. As the numerical simulation shows, the calculated neutron flux Φ in the sample position for a compact neutron source is not inferior in its values to the neutron fluxes Φ for medium-power reactors and pulsed sources, like the IBR-2 at JINR.

FUNDING

The study was supported by the Ministry of Science and Higher Education of the Russian Federation under Agreement no. 075-15-2022-830 of May 27, 2022 (continuation of Agreement no. 075-15-2021-1358 of October 12, 2021).

CONFLICT OF INTEREST

The authors declare that they have no conflicts of interest.

REFERENCES

1. Silverman, I., Arenshtam, A., Berkovits, D., et al., *AIP Conf. Proc.*, 2018, vol. 1962, p. 020002.
2. Furusaka, M., Sato, H., Kamiyama, T., et al., *Phys. Procedia*, 2014, vol. 60, p. 167.
3. Beyer, R., Birgersson, E., Elekes, Z., et al., *Nucl. Instrum. Methods Phys. Res., Sect. A*, 2013, vol. 723, p. 151.
4. Kobayashi, T., Ikeda, Sh., Otake, Y., et al., *Nucl. Instrum. Methods Phys. Res., Sect. A*, 2021, vol. 994, p. 165091.
5. Baxter, D., *Eur. Phys. J. Plus*, 2016, vol. 131, p. 83.
6. Ene, D., Borcea, C., Flaska, M., et al., *Proc. Int. Conf. ND*, Nice, 2007, p. 106.
7. Wei, J., Chen, H.B., Huang, W.H., et al., *Proc. PAC09*, Vancouver, 2009, p. 1.
8. Andreev, A.V., Burmistrov, Yu.M., Zuyev, S.V., et al., *Bull. Russ. Acad. Sci.: Phys.*, 2017, vol. 81, no. 6, p. 748.
9. Pavlov, K.A., Konik, P.I., Kovalenko, N.A., et al., *Crystallogr. Rep.*, 2022, vol. 67, no. 1, p. 3.
10. Niita, K., Sato, T., Iwase, H., et al., *Radiat. Meas.*, 2006, vol. 41, nos. 9–10, p. 1080.
11. Lefmann, K. and Nielsen, N.K., *Neutron News*, 1999, vol. 10, no. 3, p. 20.
12. Syromyatnikov, V.G., Grigoryeva, N.A., and Grigoryev, S.V., *J. Surf. Invest.: X-ray, Synchrotron Neutron Tech.*, 2023, vol. 17, no. 7, p. 818.
13. Moskvina, E.V., Grigoryeva, N.A., Kovalenko, N.A., and Grigoryev, S.V., *J. Surf. Invest.: X-ray, Synchrotron Neutron Tech.*, 2023, vol. 17, no. 7, p. 804.
14. Pavlov, K.A., Kovalenko, N.A., Azarova, L.A., et al., *J. Surf. Invest.: X-ray, Synchrotron Neutron Tech.*, 2023, vol. 17, no. 7, p. 810.
15. Barabin, S.V., Kropachev, G.N., Lukashin, A.Yu., et al., *Tech. Phys. Lett.*, 2021, vol. 47, p. 485.
16. Kropachev, G., Kulevoy, T., and Sitnikov, A., *J. Surf. Invest.: X-ray, Synchrotron Neutron Tech.*, 2019, vol. 13, no. 6, p. 1126.
17. Subbotina, V.V., Pavlov, K.A., Kovalenko, N.A., et al., *Nucl. Instrum. Methods Phys. Res., Sect. A*, 2021, vol. 1008, p. 165462.
18. <http://flnph.jinr.ru/ru/facilities/ibr-2/instruments>.
19. Grigoriev, S.V., Runov, V.V., and Okorokov, A.I., *Nucl. Instrum. Methods Phys. Res., Sect. A*, 1997, vol. 384, nos. 2–3, p. 451.
20. Syromyatnikov, V.G., Ulyanov, V.A., Lauter, V., et al., *J. Phys.: Conf. Ser.*, 2014, vol. 528, p. 012021.
21. Kashchuk, A.P. and Levitskaya, O.V., *Tech. Phys.*, 2020, vol. 65, no. 4, p. 493.
22. Meshkov, I.V., Kuznetsov, S.P., Potashev, S.I., et al., *Bull. Russ. Acad. Sci.: Phys.*, 2020, vol. 84, no. 4, p. 382.

Translated by M. Samokhina